Influence of a Heterogeneous Al$_2$O$_3$ Surface on the Electronic Properties of Single Pd Atoms

N. Nilius, T. M. Wallis,* and W. Ho†

Department of Physics and Astronomy and Department of Chemistry, University of California, Irvine, California 92697-4575
(Received 2 May 2002; published 30 January 2003)

Electronic properties of single Pd atoms, deposited on Al$_2$O$_3$/NiAl(110), have been characterized by scanning tunneling spectroscopy at 12 K. The spectra reveal distinct conductivity resonances, assigned to discrete electronic levels in the atom. The energy position of the resonances reflects adsorption properties of Pd atoms on different sites of the oxide support. Mapping the spatial extent of conductivity channels in the Pd atoms yields the symmetry of the underlying electronic states. The results demonstrate the effect of a heterogeneous oxide surface on the electronic structure of adsorbed metal atoms.

The physics and chemistry of metal-oxide interfaces are decisively determined by the defect structure of the oxide support. An oxide defect presents an unsaturated binding site, which may be active in a catalytic reaction [1,2]. More often, defects serve as nucleation centers for metal atoms and small particles, which then catalyze chemical reactions on the surface [3–5]. A detailed knowledge of the interaction between oxide defects and metal atoms is therefore necessary for the understanding and optimization of the catalytic activity of metal-oxide systems.

Large band gaps in many oxides usually prevent the formation of strong bonds to metal overlayers [6–8]. Unsaturated electronic states associated with structural defects on the oxide surface dramatically increase the binding potential and enhance metal-oxide interactions. The bond formation at oxide defects strongly affects the electronic properties of deposited metal atoms [9–11]. Residual charge trapped in defect states can be transferred to the atoms and causes a reorganization of their electronic states. As a consequence of the interaction, intrinsic adsorption and reaction properties of these atoms differ considerably from species adsorbed on defect-free oxide surfaces. For example, the unexpected catalytic activity of ultrasmall Pd or Au clusters in the CO oxidation has been partly attributed to point defects in the MgO support [12,13].

The experimental exploration of oxide defects has greatly benefited from the introduction of thin oxide films grown on metal surfaces [14–16]. Because of their transparency for low energy electrons, oxide layers are accessible to electron-mediated experimental techniques, avoiding the charging problems of insulating bulk oxides. Using photoelectron and infrared absorption spectroscopy, the effect of oxide defects on the electronic and adsorption properties of metal-oxide systems has been characterized on a mesoscopic length scale. The local defect structure was studied with electron microscopy and scanning tunneling microscopy (STM) by imaging small metal particles decorating the defects [17,18].

These experiments revealed the importance of zero- and one-dimensional defects for the nucleation and growth on oxide surfaces, but could not demonstrate their influence on the electronic properties of metal aggregates. In the experiments reported here, STM and scanning tunneling spectroscopy (STS) were combined for a topographic and electronic characterization of a metal-oxide system at the atomic level. An electronic resonance in individual Pd atoms shifts for bonding on regular and defect sites of an Al$_2$O$_3$ thin film. The experiments not only provide a local probe for the microscopic defect structure of the oxide surface, but also demonstrate the influence of defects on the electronic properties of deposited metal atoms.

The experiments were carried out in an ultrahigh-vacuum STM, operated at 12 K [19]. The NiAl(110) surface was prepared by cycles of Ne$^+$ sputtering and annealing to 1300 K. The crystal was then exposed to 180 L of oxygen at 700 K. Further annealing to 1300 K led to the formation of large, well ordered Al$_2$O$_3$ islands, covering 50% of the surface [14]. The crystalline structure of the oxide film was verified by the appearance of characteristic domain boundaries in topographic STM images [Figs. 1(a) and 1(b)]. The boundaries separate two kinds of Al$_2$O$_3$ domains, tilted by ±24° with respect to the [1$\bar{1}$0] direction of the NiAl lattice [Fig. 1(c)]. Pd atoms were evaporated from a crucible and deposited on the surface at 12 K to suppress nucleation. Atom densities on the NiAl surface are approximately 3 times larger than on oxide islands, reflecting the higher Pd sticking coefficient on the bare metal [Fig. 1(a)]. Single Pd atoms appear as protrusions in topographic images, however, with large differences in their apparent height on metal and oxide areas. On NiAl(110), the atoms are uniformly imaged as 1.3 Å high protrusions, which is close to the geometric value of a metal atom bound to a Ni row [Fig. 1(c)]. In contrast, the apparent height of Pd atoms on Al$_2$O$_3$ is 4.0 Å and varies by ±1 Å between different atoms. The height increase is independent of the metal coverage and cannot be explained by the nucleation of atoms. Oxide-supported Pd
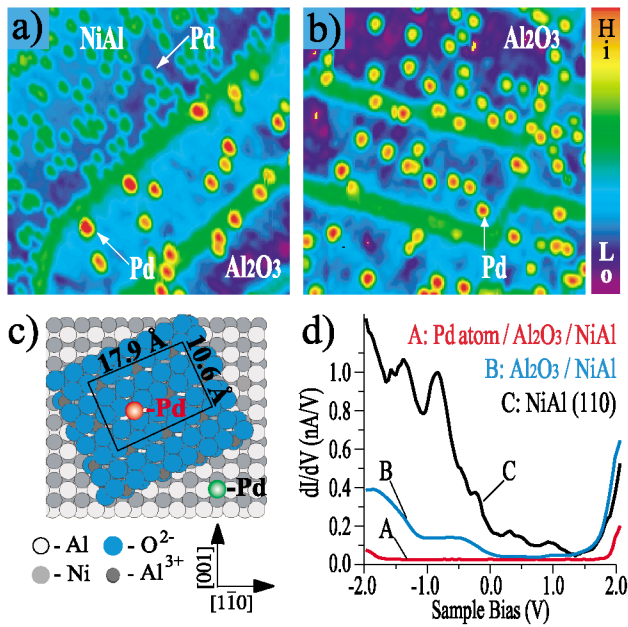
FIG. 1 (color). STM topographic images of Pd atoms on (a) NiAl (upper left corner) and (a),(b) Al_2O_3/NiAl. Oxide domain boundaries appear as green lines (375 Å × 375 Å, $V_{sample} = 3.1$ V, $I = 0.1$ nA). (c) Structure model of the Al_2O_3 unit cell on NiAl(110). (d) dI/dV spectra of the bare and oxidized NiAl surface and of a single Pd atom on Al_2O_3/NiAl.

atoms could be imaged only at sample voltages above 2.0 V, whereas no restrictions were found for the bare metal surface. Lowering the bias resulted in a removal of Pd atoms from Al_2O_3 islands during the scan.

The electronic properties of Pd atoms on the oxide support were investigated by STS. Conductivity spectra were obtained by detecting the derivative of the tunneling current (dI/dV) with a lock-in technique and provide a measure of the density of states (DOS) of the sample surface. The dI/dV spectra of bare NiAl are dominated by a distinct peak at −0.8 V and a steep increase in conductivity below −1.6 V [Fig. 1(d)]. The feature at −0.8 V can be assigned to an occupied d-like surface state, characterized by a high DOS at the surface [20]. The enhanced conductivity below −1.6 V coincides with the onset of the NiAl d bands. The growth of an Al_2O_3 film suppresses the NiAl surface state and removes the conductivity peak at −0.8 V from dI/dV spectra [Fig. 1(d)]. Because of a negligible electron density in the 8 eV oxide band gap, the underlying metal provides most of the initial and final states for tunneling, and oxide-related features are absent [14]. Positioning the tip above a Pd atom on the Al_2O_3 support further increases the tip-NiAl separation and minimizes the conductivity in the tunnel junction. No empty or occupied states are available in the range between −2.0 and 2.0 V. The atom is insulating, which explains its instability in low bias scans.

Stable imaging conditions above 2.0 V suggest Pd related electronic levels at higher energies. Extending the STS bias range reveals indeed strong Gaussian shaped conductivity resonances around 3.0 V for oxide-supported Pd atoms [Fig. 2(a)] [21]. For tip positions above the clean oxide, the peaks vanish and diodelike dI/dV curves are obtained [Fig. 2(b)]. The conductivity peaks are attributed to resonant tunneling through discrete electronic states in the Pd atom. Because of the large tip-NiAl separation and a negligible DOS in the oxide band gap, the tunneling probability is small until the Fermi level of the tip matches a Pd state [Fig. 3(a)]. Above the resonance, the conductivity in the tunnel junction decreases again and negative differential resistance is observed for some Pd atoms [Fig. 2(b), inset]. Resonant tunneling is detected only for empty Pd states at positive sample bias. Tunneling out of occupied states is unfavorable, as it involves the removal of electrons from a Pd orbital and its refilling from NiAl states in a two-step process. Additionally, the tunneling probability from filled states decreases with energy separation from the Fermi level, which complicates their detection in STS. The experimental bias position of Pd resonances is affected by the electric field in the tunnel junction, which bends the oxide bands and changes the potential at the atom site with respect to zero bias conditions [Fig. 3(a)]. Because of the high polarizability and small thickness of
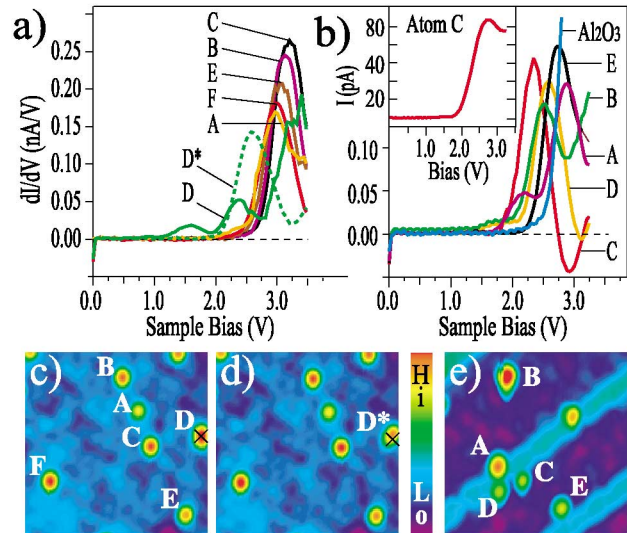

FIG. 2 (color). (a) dI/dV spectra and (c) STM topographic image of Pd atoms dosed at 12 K on Al_2O_3/NiAl (175 Å × 175 Å). Atoms mainly adsorb inside Al_2O_3 domains. (d) Surface as in (c) after manipulating atom D with the STM tip. (b) dI/dV spectra and (e) STM topographic image of Pd atoms dosed at 50 K on Al_2O_3/NiAl (200 Å × 200 Å). Atoms mainly adsorb on Al_2O_3 domain boundaries. The inset shows the I-V curve of atom C, exhibiting negative differential resistance. The tunneling gap was set with $V_{sample} = 3.0$ V, $I = 0.1$ nA.
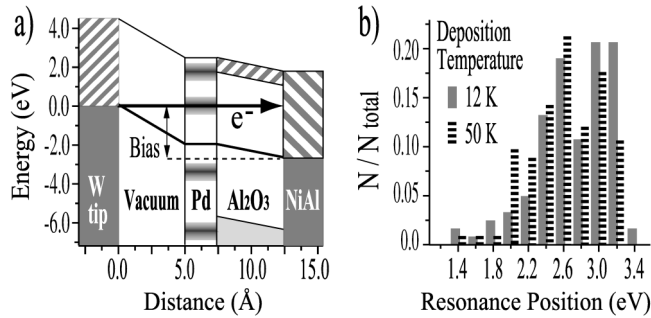
FIG. 3. (a) Potential diagram of the tunnel junction formed by a W tip and a Pd atom on Al_2O_3/NiAl, illustrating resonant tunneling through a discrete Pd electronic state. (b) Histogram of dI/dV resonance positions for 287 Pd atoms, deposited at 12 and 50 K on Al_2O_3/NiAl.

the Al_2O_3 film, deviations are expected to be small. The intrinsic resonance width of approximately 0.35 eV indicates a distinct interaction between Pd atom and oxide surface. Its delocalized character in the tip-sample junction points to an electronic state with Pd $5s$, p character [22].

Conductivity spectra shown in Fig. 2(a) are characteristic for Pd atoms on large Al_2O_3 domains. All spectra are dominated by resonances around 3.0 V, although their exact position and width changes from atom to atom. These variations are also reflected in the different appearance of atoms in topographic images [Fig. 2(c)]. The dI/dV signature obviously reflects Pd binding properties at different adsorption sites on the Al_2O_3 film. To support this assumption, the STM tip was used to move atoms between different sites, as shown for atom D [Figs. 2(c) and 2(d)]. Decreasing the sample bias to 1.0 V and ramping the current to 5.0 nA triggered a jump of the atom to a new position, accompanied by a drastic change of its conductivity spectrum [Fig. 2(a), spectrum D, D^*]. Conductivity resonances around 3.0 V were mainly observed for Pd atoms on large oxide domains, away from domain boundaries. These peaks may therefore be indicative for Pd adsorption on regular oxide sites. The variations in peak energies around 3.0 eV are attributed to the presence of different binding sites in the oxide unit cell, such as on-top and hollow positions with varying relations to neighboring Al^{3+} ions [Fig. 1(c)]. No atomic resolution of the oxide film could be obtained, which makes a differentiation of regular adsorption sites on the Al_2O_3 film not feasible from the experimental data.

The correlation between the electronic signature of single Pd atoms and their binding properties on the oxide film is further supported from an analysis of dI/dV peak positions in several hundred atoms [Fig. 3(b)]. For Pd deposition at 12 K on Al_2O_3/NiAl(110), the histogram reveals the two most probable energies for Pd atomic resonances. The maximum around 3.0 V reflects Pd adsorption inside oxide domains and suggests binding to

regular oxide sites. A second peak in the histogram around 2.5 V represents Pd atoms mainly found along oxide domain boundaries. Conductivity peaks in this energy range may therefore indicate Pd adsorption on defect sites, either line defects separating two oxide domains or point defects in the Al_2O_3 surface. Defect sites provide higher binding energies, which modifies the Pd-oxide interaction and affects the electronic signature of Pd atoms [9,10]. To test the correlation between Pd resonances at 2.5 V and defect adsorption, the occupation of defect sites was influenced by enabling Pd diffusion. At a deposition temperature of 50 K, Pd atoms have longer trajectories on the surface and are more likely trapped on oxide defects than at 12 K. As expected, more atoms were observed on domain boundaries of the Al_2O_3 film [Fig. 2(e)]. Conductivity spectra of the corresponding Pd atoms are dominated by resonances around 2.5 V, although peak positions are scattered in a wider energy range [Fig. 2(b)]. In the energy histogram obtained from deposition experiments at 50 K, the low energy peaks clearly gain weight at the expense of resonances around 3.0 V [Fig. 3(b)]. The result supports an interrelation between redshifted Pd resonances and adsorption on defect sites of the Al_2O_3 film. An additional maximum around 2.0 V in the histogram is attributed to small Pd aggregates and marks the onset of nucleation for high temperature deposition.

Conductivity images can provide information on the spatial extent of electronic resonances by mapping the dI/dV signal at the peak position. Figure 4(b) displays conductivity images for three Pd atoms on Al_2O_3 in addition to their dI/dV spectra [Fig. 4(a)]. Atom A, adsorbed on a regular oxide site, shows a 3.1 V resonance with circular symmetry [Fig. 4(b), A]. The shape of the conducting channel might be indicative for an s symmetry of the corresponding Pd orbital. Above the resonance energy, the dI/dV signal of the atom decreases
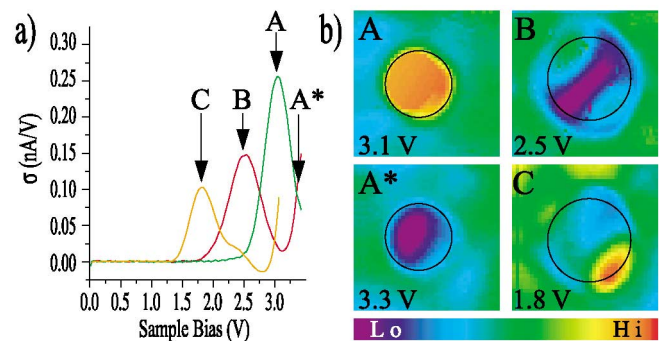

FIG. 4 (color). (a) dI/dV spectra and (b) conductivity images of three Pd atoms on different Al_2O_3 adsorption sites (35 Å × 35 Å, $I = 0.1$ nA). To compare the spatial distribution of conducting channels, the apparent size of atoms in topographic images is marked by circles.

below the level of the surrounding oxide and leaves a depression at the atom site [Fig. 4(b), A^*]. The image of the electronic resonance at 2.5 V in atom B is dominated by a nodal plane in the center of the conducting channel [Fig. 4(b), B]. Its different shape compared to resonances around 3.0 V may reflect interactions between the Pd orbital and oxide defect states. The 1.8 V resonance of atom C is characterized by an asymmetric spatial distribution [Fig. 4(b), C]. The low energy and the unusual symmetry of the conducting channel suggest strong coupling to a local defect underneath the atom.

The results on the electronic properties of single Pd atoms on Al_2O_3/NiAl(110) can be compared with theoretical models describing the bonding of metal atoms to oxide surfaces. For sapphire and Al_2O_3 films on Al(111) and Ru(0001), density functional theory calculations predict strong binding of single transition metal atoms [23]. The adsorption is accompanied by a charge transfer from the atom to the oxide and yields binding energies of 3.2 eV for Pd atoms on Al_2O_3 hollow sites [24]. In contrast, the Pd binding to MgO(0001) has mainly been attributed to electrostatic interactions induced by the oxide Madelung field and leads to adsorption energies of approximately 1.0 eV [22,25]. The binding strengthens dramatically for Pd atoms at oxygen vacancies in the MgO surface [10]. The stability of Pd atoms in our experiment points to a considerable binding energy on regular and defect Al_2O_3 sites, but does not allow any quantitative estimation of the interaction strength. Following the theoretical predictions, the observed unoccupied state in Pd atoms is tentatively assigned to the Pd $5s$ orbital. Although this state is also empty in the free atom, the unknown occupation of the Pd d levels in this experiment prevents a determination of the possibility of charge transfer in the binding process. The shift of the Pd resonance towards the Fermi level for an adsorption on oxide defect sites is in agreement with a gradual filling of the Pd $5s$ orbital, as calculated for Pd adsorption on color centers of MgO(0001) [10]. The position of the Pd resonance is a sensitive probe of the oxide adsorption site and can, therefore, be used to test different binding models by comparing experimental and calculated resonance energies.

The present study demonstrates the influence of local defects on an Al_2O_3 surface on the electronic properties of single Pd atoms. The approach should be applicable to other metal-oxide systems, providing necessary information to refine existing models of metal-oxide interactions. Because of their heterogeneous and complex structure, oxide surfaces are in general challenging for theory and experiment. However, the importance of metal-oxide systems in various technologies, such as electronics and catalysis, warrants a continuing effort toward their characterization on the atomic scale.

*On leave of absence from Department of Physics, Cornell University, Ithaca, NY 14853-2501.
†Corresponding author.
Electronic address: wilsonho@uci.edu

[1] *Handbook of Heterogeneous Catalysis*, edited by G. Ertl, H. Knözinger, and J. Weitkamp (Wiley, Weinheim, 1997).
[2] R. Schaub *et al.*, Phys. Rev. Lett. **87**, 266104 (2001).
[3] C. T. Campbell, Surf. Sci. Rep. **27**, 1 (1997).
[4] M. Valden, X. Lai, and D. W. Goodman, Science **281**, 1647 (1998).
[5] H. J. Freund *et al.*, Top. Catal. **15**, 201 (2001).
[6] C. Noguera, *Physics and Chemistry at Oxide Surfaces* (Cambridge University, Cambridge, 1996).
[7] K. Højrup Hansen *et al.*, Phys. Rev. Lett. **83**, 4120 (1999).
[8] J. H. Larsen, J. T. Ranney, D. E. Starr, J. E. Musgrove, and C. T. Campbell, Phys. Rev. B **63**, 195410 (2001).
[9] N. Lopez, F. Illas, and G. Pacchioni, J. Am. Chem. Soc. **121**, 813–821 (1999); G. Pacchioni, Solid State Sci. **2**, 161 (2000).
[10] V. A. Nasluzov *et al.*, J. Chem. Phys. **115**, 8157 (2001).
[11] A. Bogicevic and D. R. Jennison, Surf. Sci. **515**, L481 (2002).
[12] A. Sanchez *et al.*, J. Phys. Chem. A **103**, 9573 (1999).
[13] S. Abbet, U. Heiz, H. Häkkinen, and U. Landman, Phys. Rev. Lett. **86**, 5950 (2001).
[14] R. M. Jaeger *et al.*, Surf. Sci. **259**, 235 (1991).
[15] S. C. Street, C. Xu, and D. W. Goodman, Annu. Rev. Phys. Chem. **48**, 43 (1997).
[16] W. Weiss and W. Ranke, Prog. Surf. Sci. **70**, 1 (2002).
[17] C. R. Hernry, Surf. Sci. Rep. **31**, 235 (1998).
[18] M. Bäumer and H.-J. Freund, Prog. Surf. Sci. **61**, 127 (1999).
[19] B. C. Stipe, M. A. Rezaei, and W. Ho, Rev. Sci. Instrum. **70**, 137 (1999).
[20] K. Højrup Hansen *et al.*, Phys. Rev. B **63**, 115421 (2001).
[21] Pd atoms on NiAl(110) show weak features at 2.8 V in dI/dV spectra. In contrast to oxide-supported atoms, peak positions and linewidths are identical for different atoms on the metal surface.
[22] K. Neyman, S. Vent, N. Rösch, and G. Pacchioni, Top. Catal. **9**, 153 (1999).
[23] C. Verdozzi, D. R. Jennison, P. A. Schultz, and M. P. Sears, Phys. Rev. Lett. **82**, 799 (1999); D. R. Jennison and A. Bogicevic, Surf. Sci. **464**, 108 (2000).
[24] A. Bogicevic and D. R. Jennison, Phys. Rev. Lett. **82**, 4050 (1999).
[25] The different structure of Al_2O_3 thin film and MgO allows only a general comparison of the Pd binding process.